A Vector Controlled High Performance Matrix Converter - Induction Motor Drive

Sadao Ishii*, Eiji Yamamoto*, Hidenori Hara*, Eiji Watanabe*, Ahmet M. Hava **, and Xiaorong Xia ***

Yaskawa Electric Corporation*
12-1 Ohtemachi, Kokura-Kita-ku, Kitakyusyu 803-8530, Japan
Phone: +81-93-571-6238, Fax +81-93-571-6028
E-mail: sada@yaskawa.co.jp

Yaskawa Electric America, Inc. **
2121 Norman Drive South
Waukegan IL 60085, U.S.A.
Phone +01-847-887-7011, Fax +01-847-887-7090
E-mail: ahmet_hava@yaskawa.com

Virginia Polytechnic Institute & State University ***
Center for Power Electronics Systems
Blacksburg, VA 24061, U.S.A.
Phone +01-540-231-5494, Fax +01-540-231-6390
E-mail: xiaxr@vt.edu

Abstract - Due to its regeneration ability and sinusoidal input current, the matrix converter is superior to the PWM inverter drives. Therefore, it meets the stringent energy-efficiency and power quality requirements of the new century. Following the strong R&D efforts over the last two decades, the matrix converter is now becoming a viable AC-to-AC direct power conversion device that is suitable for a large number of applications. This paper describes the basic operating principles and control method of the matrix converter, and reports the detailed experimental operating characteristics of an 11 kVA matrix converter drive over its full operating range. Through the experimental operating characteristics, the paper illustrates the feasibility of the matrix converter drive as an environment-friendly future-generation drive.

Key words: Displacement angle control, Harmonics, Induction Motor, Matrix Converter, Regenerative Operation, Vector Control.

1. Introduction

Supported by remarkable progress in the areas of semiconductor power devices and microelectronics, PWM inverters have rapidly matured over the last few decades. As a result, they have been dominantly employed in variable speed motor drive applications due to their superior drive performance and energy saving characteristics. However, as the number and the power ratings of such applications grew at an enormous rate, several negative attributes of the PWM inverters have become intolerable. These attributes are now commonly recognized as a major source of concern for the electric utility as well as the users of such devices.

The diode rectifier front ends of the PWM inverters feed harmonics to the utility grid and pollute the AC line such that other equipment on the same line experience interference and have operating problems such as commutation failure, EMI etc. Furthermore, the diode rectifier front end type PWM inverters have no regeneration capability and in most applications with frequent regeneration operating mode, the regenerated energy is dissipated in a resistive circuit (dynamic brake) with limited capacity. This attribute renders the drive energy inefficient and dynamically insufficient. Therefore, the energy efficiency, power quality, and dynamic performance of inverter drives are falling short of the stringent environmental, power quality, and performance demands of the new century. The matrix converter (MC) is a modern power conversion device that has been developed over the last two decades [1]-[3] and it meets all these requirements.

MC is a direct AC-AC energy conversion device with the functionality of a PWM inverter, but it is free from the harmonic pollution and regeneration problems. MC is a forced commutation converter that converts the AC line voltage to a variable-voltage variable-frequency source without using an intermediate DC link circuit, and it has the following advantages.

1. It can operate in all four quadrants of the torque-speed plane.
2. Its input current waveform is sinusoidal and the input power factor is unity.
3. It exhibits high drive performance via PWM and vector control.
4. Continuous zero speed operation is available because no current concentrates in any of the switches.
5. It has high reliability and long life due to the absence bulky electrolytic capacitors.

Following the review of the MC operating principles and description of the involved control technique, this paper describes the prototype matrix converter- induction motor drive system configuration and demonstrates its performance in detail. The paper demonstrates the static and dynamic characteristics of the MC drive in detail and illustrates its input total harmonic distortion (THD) characteristics. It illustrates the successful operating performance of MC over a wide range and verifies its feasibility as a high performance modern power electronic conversion device.

2. Control and Operating Principles

2.1. Principles

MC is a direct power conversion device that converts three-phase AC line voltages to variable-voltage variable-frequency three-phase outputs. It consists of nine bidirectional switches The switching pattern is established via a PWM technique The reference output line voltages of the pulse width modulator are generated by the outer control loop, which is a high performance vector controller (synchronous frame current controller, identical to those employed in inverter drives). Fig.1 shows the main circuit configuration of the MC drive. The voltages at the output terminals of MC are generated from the input voltages by switching over among a group of bidirectional switches ($\boldsymbol{S}_u$, $\boldsymbol{S}_v$, $\boldsymbol{S}_w$).

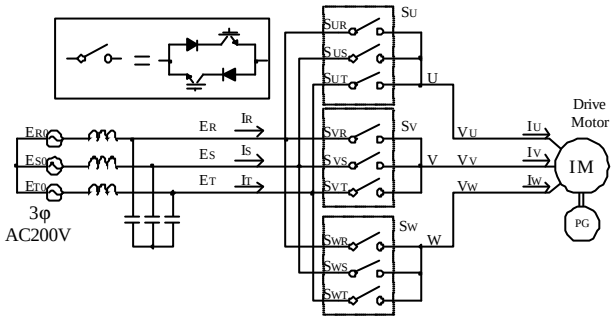

Fig. 1. Ideal model of MC.

The output phase voltages can be written by the following.

$$\begin{bmatrix} V_U \\ V_V \\ V_W \end{bmatrix} = \begin{bmatrix} \boldsymbol{S}_U \\ \boldsymbol{S}_V \\ \boldsymbol{S}_W \end{bmatrix} \begin{bmatrix} E_R \\ E_S \\ E_T \end{bmatrix} = \begin{bmatrix} S_{UR} & S_{US} & S_{UT} \\ S_{VR} & S_{VS} & S_{VT} \\ S_{WR} & S_{WS} & S_{WT} \end{bmatrix} \begin{bmatrix} E_R \\ E_S \\ E_T \end{bmatrix} \quad (1)$$

The output line voltages can be calculated from (1) in the form shown in (2), which indicates that in order to control the output line voltages, the groups of bidirectional switches $\boldsymbol{S}_u$, $\boldsymbol{S}_v$, and $\boldsymbol{S}_w$ must be selected appropriately.

$$\begin{bmatrix} V_{UV} \\ V_{VW} \\ V_{WU} \end{bmatrix} = \begin{bmatrix} S_{UR}-S_{VR} & S_{US}-S_{VS} & S_{UT}-S_{VT} \\ S_{VR}-S_{WR} & S_{VS}-S_{WS} & S_{VT}-S_{WT} \\ S_{WR}-S_{UR} & S_{WS}-S_{US} & S_{WT}-S_{UT} \end{bmatrix} \begin{bmatrix} E_R \\ E_S \\ E_T \end{bmatrix} \quad (2)$$

For safe operation of the system, the MC input terminals must not be short-circuited and the output terminals must not be open-circuited via the MC switches. These rules are expressed in the following.

$$\begin{bmatrix} S_{UR}+S_{US}+S_{UT} \\ S_{VR}+S_{VS}+S_{VT} \\ S_{WR}+S_{WS}+S_{WT} \end{bmatrix} = \begin{bmatrix} 1 \\ 1 \\ 1 \end{bmatrix} \quad (3)$$

In (1), (2), and (3), S_{UR} through S_{WT} indicate the state of the MC switches and each one takes a value of "1" or "0", which indicates that the switch is in "closed" state or in "opened" state respectively.

2.2. PWM method

The MC static characteristics are strongly dependent on the MC control method. Since MC is a device without energy storage elements (at least theoretically), its input and output behavior are strongly dependent on each other. For varying operating conditions of the output, the behavior of its input is expected to vary also. Therefore, the input power factor and input current THD of the MC depend on the load characteristics and operating point. However, with an adequate control technique, the MC input behavior can become independent of the output operating conditions. Many MC control methods have been reported in the literature [1]-[5] and for various control methods, the MC static characteristics are different. In this work, the control method in [6]-[8] has been employed. In addition to providing an improved power factor and low input current THD, this method exhibits superior performance under voltage source distortion/unbalance operating conditions.

The control technique employed in this work will be described with the aid of the simplified MC drive circuit model that is shown in Fig.2. As shown in the figure, in input side, $E_{(R,S,T)}$ and $Ii_{(R,S,T)}$ are sorted and labeled as $E_{(MIN,MID,MAX)}$, and $Ii_{(MIN,MID,MAX)}$ respectively. The sorting rule is described in Table I. In the table, $q(Ii)^*$ is the input current angle reference. The base voltage, E_{base}, is the input phase voltage that is associated with the input phase current with the largest magnitude. The output voltages and currents $V_{(U,V,W)}$ and $Io_{(U,V,W)}$ are sorted and labeled as $V_{(MIN,MID,MAX)}$, and $Io_{(MIN,MID,MAX)}$ with a similar sorting rule. This sorting rule is illustrated in Table II, where qv^* is the output voltage angle reference.

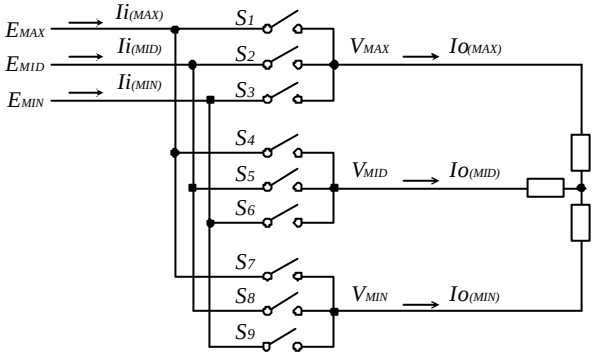

Fig. 2. Simplified model of the MC drive circuit.

Table I. Input stage sorting rules and the base voltage.

$\theta(Ii)^*$	-π/6	-π/3	-π/2	-2π/3	-5π/6	-π	-7π/6	-4π/3	-3π/2	-5π/3	-11π/6	-2π
E_{max}	E_t	E_r	E_r	E_r	E_r	E_s	E_s	E_s	E_s	E_t	E_t	E_t
E_{mid}	E_r	E_t	E_t	E_s	E_s	E_r	E_r	E_t	E_t	E_s	E_s	E_r
E_{min}	E_s	E_s	E_s	E_t	E_t	E_t	E_t	E_r	E_r	E_r	E_r	E_s
E_{base}	E_{min}	E_{min}	E_{max}	E_{max}	E_{min}	E_{min}	E_{max}	E_{max}	E_{min}	E_{min}	E_{max}	E_{max}

Table II.Output stage sorting rules.

θ_V^*	-π/6	-π/3	-π/2	-2π/3	-5π/6	-π	-7π/6	-4π/3	-3π/2	-5π/3	-11π/6	-2π
V_{max}	V_w	V_u	V_u	V_u	V_u	V_v	V_v	V_v	V_v	V_w	V_w	V_w
V_{mid}	V_u	V_w	V_w	V_v	V_v	V_u	V_u	V_w	V_w	V_v	V_v	V_u
V_{min}	V_v	V_v	V_v	V_w	V_w	V_w	V_w	V_u	V_u	V_u	V_u	V_v

The switching pattern and output line voltages over a carrier period Tc are shown in Fig. 3(A) and (B) in detail. Fig.3(A) corresponds to the case that $E_{base}=E_{MIN}$.
In this case, the switches S_7 and S_8 remain in closed and S_9 remains open over the full carrier cycle. The remaining switches S_1 through S_6 are pulse width modulated as shown in the figure. Similarly, fig. 3(B) corresponds to the $E_{base}=E_{MAX}$ case. In this case, S_2 and S_3 remain open and S_1 remains closed over Tc. The remaining switches S_4 through S_9 are pulse width modulated as shown in the figure. In order to simplify the formulas involved in the duty cycle computation of each switch, the terms ΔE_{MAX} , ΔE_{MID} , ΔV_{MAX}, and ΔV_{MID} are defined in the following.

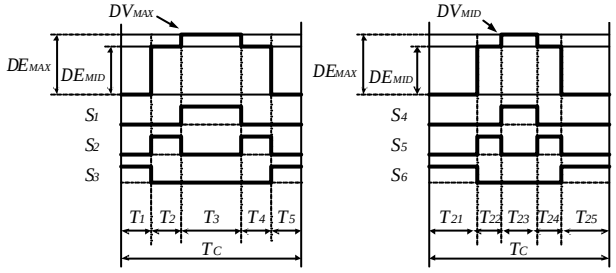

(A) Case 1 (S_7=S_8=0,S_9=1)

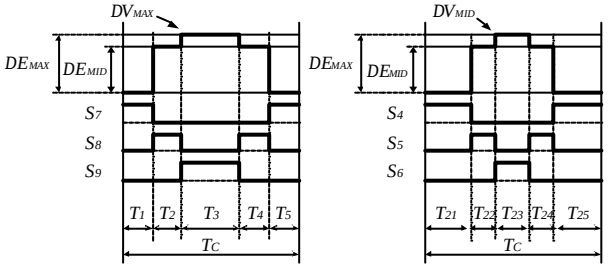

(B) Case 2 (S_1=1,S_2=S_3=0)

Fig.3. Switching pattern for cases (A) and (B).

$$\Delta E_{MAX} = E_{MAX} - E_{MIN} \tag{4}$$

$$\Delta E_{MID} = \begin{Bmatrix} E_{MAX} - E_{MID}; E_{base} = E_{MAX} \\ E_{MID} - E_{MIN}; E_{base} = E_{MIN} \end{Bmatrix} \tag{5}$$

$$\Delta V_{MAX} = V_{MAX} - V_{MIN} \tag{6}$$

$$\Delta V_{MID} = \begin{Bmatrix} V_{MAX} - V_{MID}; E_{base} = E_{MAX} \\ V_{MID} - V_{MIN}; E_{base} = E_{MIN} \end{Bmatrix} \tag{7}$$

The per carrier cycle average value of output line voltages can be obtained as

$$\Delta V_{MAX} = \frac{1}{T_C}\{(T_2 + T_4)\cdot \Delta E_{MID} + T_3 \cdot \Delta E_{MAX}\} \tag{8}$$

$$\Delta V_{MID} = \frac{1}{T_C}\{(T_{22} + T_{24})\cdot \Delta E_{MID} + T_{23} \cdot \Delta E_{MAX}\} \tag{9}$$

where $T_C = T_1 + T_2 + T_3 + T_4 + T_5 = T_{21} + T_{22} + T_{23} + T_{24} + T_{25}$.

Under these conditions, input currents Ii(min,mid, max) can be written in the following.

$$Ii_{(ch)} = \frac{1}{T_C}\{T_3 \cdot Io_{(ch)} + T_{23} \cdot Io_{(MID)}\} \tag{10}$$

$$Ii_{(MID)} = \frac{1}{T_C}\{(T_2 + T_4)\cdot Io_{(ch)} + (T_{22} + T_{24})\cdot Io_{(MID)}\} \tag{11}$$

where $ch=MAX$ at $E_{base}=E_{min}$, $ch=MIN$ at $E_{base}=E_{max}$.

By selecting the time intervals T_1 through T_5 and T_{21} through T_{25}, any arbitrary value of output voltage can be created. The input current distribution factor, α is defined as follows.

$$a = \frac{T_2 + T_4}{T_3} = \frac{T_{22} + T_{24}}{T_{23}} = Ii_{(MID)} / Ii_{(ch)} \tag{12}$$

Using α, (8)-(9) can be re-written in the following.

$$T_3 = T_C \cdot \frac{\Delta V_{MAX}}{a \cdot \Delta E_{MID} + \Delta E_{MAX}} \tag{13}$$

$$T_{23} = T_C \cdot \frac{\Delta V_{MID}}{a \cdot \Delta E_{MID} + \Delta E_{MAX}} \tag{14}$$

Choosing α as a function of *q(Ii)** from Table I, sinusoidal input currents can be generated. The output line voltages can be controlled with the variables T_3, T_2+T_4, T_{23}, and T_{22}+T_{24}. The variables T_1 , T_2, T_4, T_5, T_{21}, T_{22}, T_{24} and T_{25} can be freely selected.

2.3. Displacement angle control

The phase angle of the input currents can be displaced by DE_{MAX}, and DE_{MID} and a based on the input current angle reference *q(Ii)**.

Fig.4(A) shows DE_{MAX}, DE_{MID}, a and input current when *q(Ii)** is equal to the input voltage angle q_E. Similarly, Fig.4(B) shows DE_{MAX}, DE_{MID}, a and input current when *q(Ii)**, is equal to $q_E + p/12$.

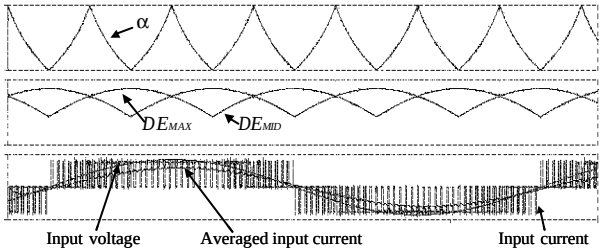

(A) $q(Ii)^*=q_E$

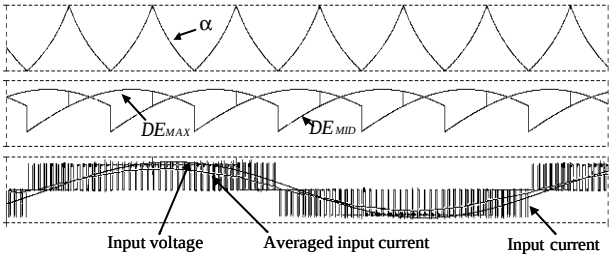

(B) $q(Ii)^*=q_E+p/12$

Fig.4. Input voltage and input current waveforms.

3. System Configuration

Fig.5 illustrates the main control block diagram of the experimental MC drive system. The "Matrix Converter" block includes the LC input filters and nine bidirectional switches. The LC input filters are for filtering the carrier freqency components. Each bidirectional switch consists of two antiparallel IGBTs and diodes. The MC drive is connected to an induction motor with shaft encoder. The MC drive and induction motor nameplate data is given in Table III. The induction motor is coupled with an inertial load and a dynamometer.

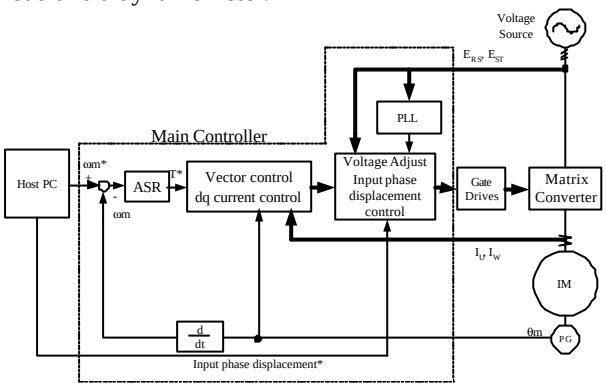

Fig.5. MC drive system detailed control diagram.

Table III. Experimental system nameplate data.

Matrix converter	11 kVA, 200 V, 33 A
Induction motor	7.5 kW, 33 A, 1800 r/min, 4 poles
Inertia	0.315 kg-m^2

The motor controller employs the state of the art vector control technique (field orientation). The vector controller utilizes the speed reference and feedback signals to generate the d-q frame reference currents. The synchronous frame d-q current regulator utilizes the reference and feedback currents to generate the voltage reference signals for the MC controller. The reference voltages are processed in the MC controller that generates the pulse pattern for the MC switches. The input displacement angle control is implemented in the main controller by *q(Ii)**. All the control loops have been implemented on a Digital Signal Processor (DSP) platform by means of software programs. The shaft encoder signal, motor currents, input voltages and the phase information of the input line voltages are all input into the DSP. The system is operated via a host PC.

4. Experimental Results

In this section, the superior performance of the prototype MC drive will be demonstrated via experimental data. Both the steady state operating characteristics and the dynamic operating performance will be demonstrated and the results discussed.

4.1 Torque characteristic

The torque linearity characteristics of the drive were measured under steady state operating conditions (and at fixed motor frame temperature). Fig.6 shows the linearity between the reference torque and the actual torque. It indicates that the vector controlled MC drive torque regulation capability is high (the tolerance of torque is within ±5% of the rated torque). Therefore, the torque regulation performance of the vector controlled MC drive matches the performance of the vector controlled PWM inverter drive.

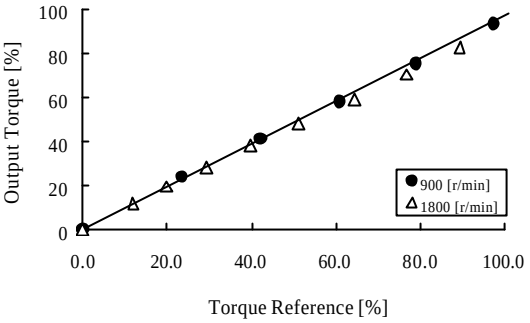

Fig. 6. Torque linearity of vector controlled MC drive.

4.2 Displacement angle control and input output waveforms

Fig.8. shows relation between the load torque and the input power factor and THD with and without input displacement angle control. Rated speed, and half-rated speed were considered. The graphs illustrate that at partial load the power factor is significantly improved. The input current THD remains low in all the operating range with and without input displacement angle control. It only slightly increases under no-load operating condition. Under all the operating conditions it remained under 10% illustrating excellent performance when compared to diode-rectifier front-end type PWM inverter drives.

Fig.7 shows the input phase voltages and currents, output line voltages and phase current for MC drive with and without input displacement angle control. The waveforms correspond to 900r/min (50 % of rated speed), 19.9Nm (50 % of rated torque) operating condition. With input displacement angle control, the power factor could be made unity so that MC drive power quality and kW/volume rating become excellent.

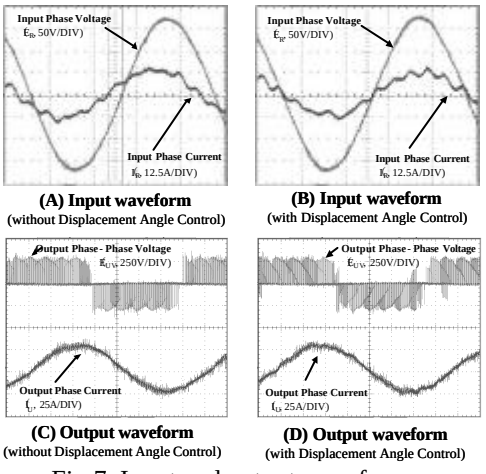

Fig.7. Input and output waveforms.

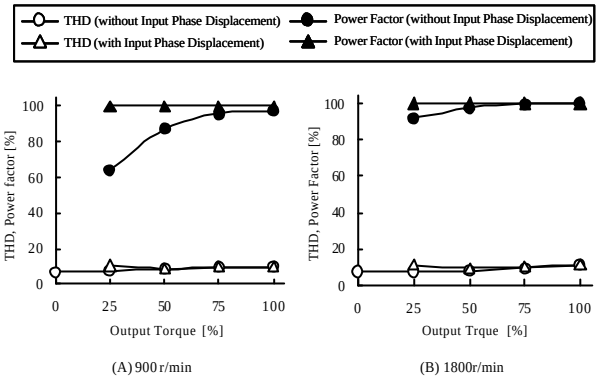

Fig.8. Power factor and THD of the input current.

4.3 Four quadrant operation

Fig.9 shows the four quadrant operation characteristics. The inertial load was accelerated to ±1800 r/min with a speed reference with step function. Therefore, the drive operates at the peak torque (current) capability during acceleration and deceleration. The linear acceleration and deceleration graphs of Fig. 9 indicate that during acceleration/deceleration the reference torque is constant. The waveforms indicate that the speed reversal and change over from motoring to the regenerating mode is achieved smoothly. During regeneration, except for the small MC switching losses, most of the inertial energy is immediately (and directly) returned to the AC line. Thus, in all the four quadrants, high energy-efficiency and very rapid speed response could be achieved.

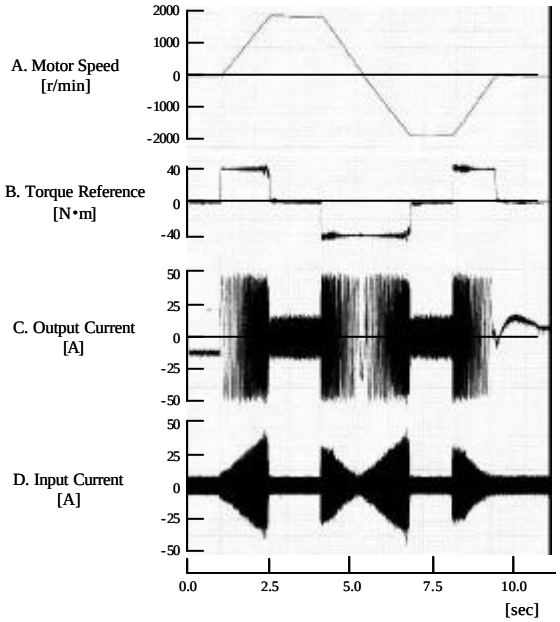

Fig. 9. Four quadrant operation waveforms.

4.4 Speed step response

The speed response of the drive was measured by applying a step increase and then a step decrease to the speed reference signal. The operating speed for this test was selected as 800 r/min. Fig. 10 shows the 60 r/min speed step response. In both cases, the actual speed rapidly reaches the reference and stabilizes within 100ms. Thus, the drive exhibits favorable speed response characteristics. Notice that during speed transients, the reference torque rapidly increases so that the energy that is necessary to regulate the system speed is rapidly transferred from (to) the motor to (from) the AC line.

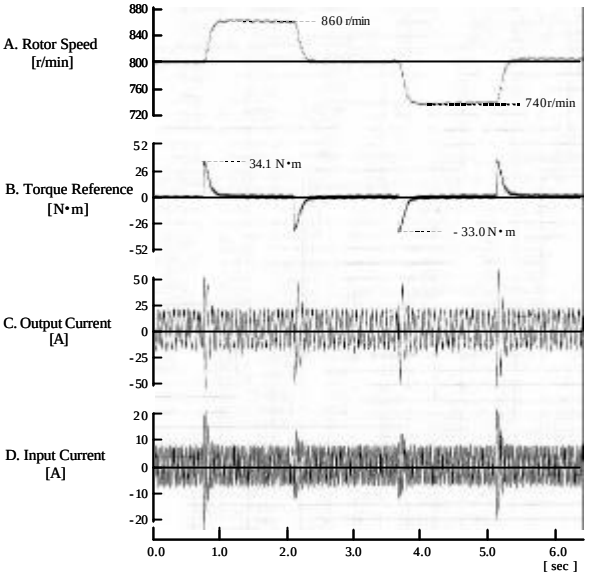

Fig.10. Speed step response.

4.5 Impact load response

In order to demonstrate the rapid torque response of the MC drive, while operating at 800 r/min speed, the load torque was rapidly stepped up from 20% of the rated torque to 75% in both motoring (A) and regenerating (B) directions. Fig. 11 illustrates that in both cases the speed drop/overshoot is approximately 1.5% of the rated speed. The waveforms indicate that unlike the PWM inverter drive power control characteristics, the MC power control characteristics are symmetric for motoring and regenerating operating conditions. The rapid response under impact loading conditions illustrates that the MC drive has a superior dynamic performance.

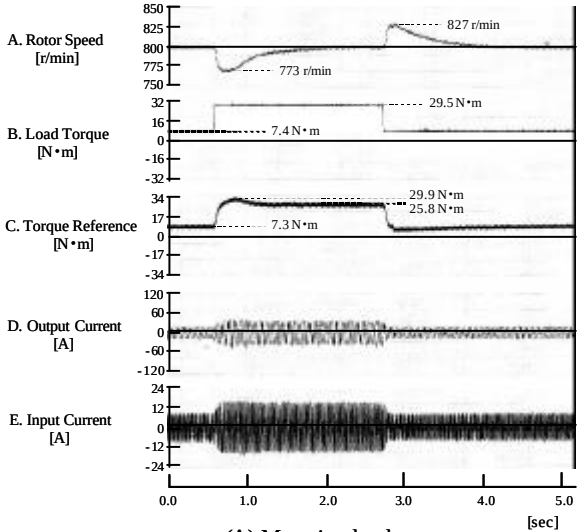

(A) Motoring load

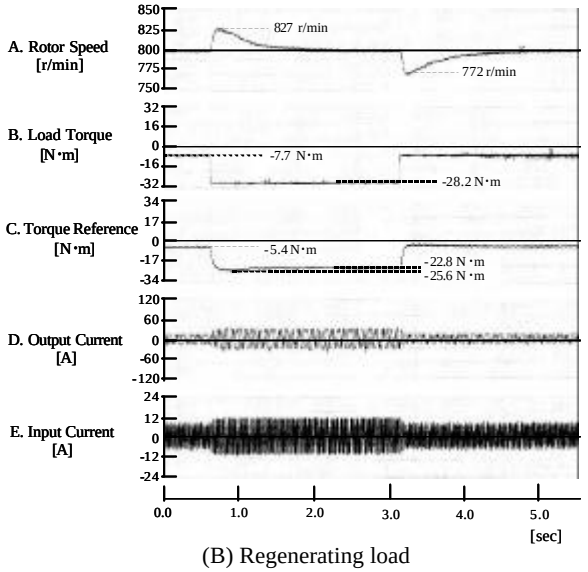

(B) Regenerating load

Fig.11. Impact load response for motoring (A) and regenerating (B) conditions.

5. Conclusions

The superior overall performance characteristics of an MC drive have been demonstrated via experimental results of a prototype drive. An MC has been built and utilized to drive a vector controlled induction motor with inertia load. A modulation technique with superior performance has been utilized. Experimental results illustrate that in addition to the full controllability of the MC output voltage, this technique also yields near unity power factor and high waveform quality at the input.

Steady state and dynamic transient operating characteristics have been obtained over a wide operating range by detailed experiments of the prototype. The following important conclusions can be reached from these results.

1) The steady state attributes such as the speed regulation, torque capability, etc. of the MC drive match those of the PWM inverter drive. In addition, the vector controlled MC drive exhibits significantly better speed step-response and impact-load response. The four quadrant operating capability results in significantly wider dynamic performance.
2) Under all the normal speed and voltage operating conditions, a near unity power factor could be achieved. The input current is sinusoidal and has a significantly lower THD than the diode rectifier front-end type PWM inverter drives.
3) Due to the four quadrant operating capability, the energy efficiency of the MC drive is superior to the PWM inverter. During regenerative operation, most of the load energy is returned to the input source. The only losses are the power semiconductor losses and input filter losses (comparable to the PWM inverter semiconductor losses, accounting for the front-end diode rectifier losses also) that are small compared to the regenerated energy. Thus, a very high overall energy efficiency could be obtained.

With its superior performance over the state of the art PWM inverter drives proven, the matrix converter is rapidly progressing towards becoming the modern power conversion device of the new century. Due to its superior energy efficiency and power quality and smaller physical size, the MC drive is the strongest candidate to meet the stringent "clean environment" requirements of the modern society. Thus, the authors wish to immediately apply the technology in regenerative drive applications and then rapidly spread its application fields. Further work involving the input power quality improvement is in progress.

References

[1] M. Venturini, "A New Sine Wave In Sine Wave out, Conversion Technique Which Eliminates Reactive Elements," , Proceedings Powercon 7 , pp.E3-1-E3-15, 1980.

[2] P. D. Ziogas, S. I. Khan, and M. H. Rashid, "Analysis and design of forced commutated cycloconverters structures with improved transfer characteristics," IEEE Trans. on industrial electronics, vol. IE-33, no 3, August 1986.

[3] A. Alesina and M. Venturini, "Intrinsic amplitude limits and optimum design of 9-switches direct PWM AC-AC converters," Conf. Record, IEEE-PESC 1988, pp. 1284-1291.

[4] L. Huber and D. Borojevic, "Space Vector Modulated Three-Phase to Three-Phase Matrix Converter with Input Power Factor Correction," IEEE Trans. On Industry Application, vol. 31, No.6, pp.1234-1246, Nov.1995.

[5] A. Ishiguro, T. Furuhashi, M. Ishida, and S. Okuma, "Output Voltage Control Method for PWM-Controlled Cycloconverters Using Instantaneous Values of Input Line to Line Voltages," IEEJ, vol.111-D, No.3, pp.201-207, 1991.

[6] J. Oyama, X. Xia, T. Higuchi, K. Kuroki, E. Yamada, and T. Koga, "A New On-line Gate Curcuit for Matrix Converter," in IPEC-Yokohama Conf. Rec., Yokohama, Japan, 1995, pp. 754-758.

[7] J. Oyama, X. Xia, T. Higuchi, and E. Yamada, "Displacement Angle Control for Matrix Converter," Conf. Rec. of PESC'97 IEEE, pp.1033-1039, June 1997.

[8] S. Ishii, E. Yamamoto, H. Hara, E. Watanabe, X. Xia, and J. Oyama, "Characteristic of Matrix Converter under Vector Control driven IM," Proceedings of ISA JIASC'99, vol.3, pp.163-166, Aug, 1999.